

Nuclear design of a shielded cabinet for electronics: the ITER Radial Neutron Camera case study

F. Moro^{a*}, D. Marocco^a, F. Belli^a, G. Brolatti^a, C. Centioli^a, A. Colangeli^a, G. Di Mambro^b, D. Flammini^a, N. Fonnese^a, G. Gandolfo^a, R. Kantor^c, J. Kotula^c, A. Maffucci^b, G. Mariano^a, D. Marzullo^d, R. Ortwein^c, S. Podda^a, F. Pompili^a, M. Riva^a, Dustin Sancristóbal^e, R. Villari^a and B. Esposito^a

^aENEA, Department of Fusion and Nuclear Safety Technology, I-00044, Frascati, Rome, Italy

^bUniversity of Cassino and Southern Lazio, Electrical and Information Engineering Dept., 03043 Cassino (Fr), Italy

^cInstitute of Nuclear Physics of the Polish Academy of Sciences, ul. Radzikowskiego 152, 31-342 Cracow, Poland

^dTrieste University, Department of Engineering and Architecture, 34127, Trieste, Italy

^eIDOM s.a., Av. de la Fama, 11-15, 08940, Cornellàde Llobregat, Barcelona, Spain

*Corresponding author: fabio.moro@enea.it

The Radial Neutron Camera (RNC) is a diagnostic located in ITER Equatorial Port #1 providing several spatial and time-resolved parameters for fusion power estimation, plasma control and physics studies. The RNC measures the uncollided 14 MeV and 2.5 MeV neutrons from deuterium-tritium (DT) and deuterium-deuterium (DD) fusion reactions through an array of neutron flux detectors located in collimated Lines of Sight. Signals from RNC detectors (fission chambers, single Crystal Diamonds and scintillators) need preamplification because of their low amplitude. These preamplifiers have to be as close as possible to the detectors in order to minimize signal degradation and must be protected against fast and thermal neutrons, gamma radiation and electromagnetic fields.

The solution adopted is to host the preamplifiers in a shielded cabinet located in a dedicated area of the Port Cell, behind the Bioshield Plug.

The overall design of the cabinet must ensure the necessary magnetic, thermal and nuclear shielding and, at the same, satisfy weight and allocated volume constraints and maintain its structural integrity. The present paper describes the nuclear design of the shielded cabinet, performed by means of 3D particle transport calculations (MCNP), taking into account the radiation streaming through the Bioshield penetrations and the cross-talk effect from the neighboring Lower and Upper Ports. We present the assessment of its nuclear shielding performances and analyze the compliancy with the alert thresholds for commercial electronics in terms of neutron flux and cumulated ionizing dose.

Keywords: neutron diagnostics, Radial Neutron Camera, ITER, neutronics, electronics, MCNP

1. Introduction

The Radial Neutron Camera (RNC) [1] is a key ITER diagnostic system hosted in the Equatorial Port #1 (EP01), designed to detect 14 MeV and 2.5 MeV uncollided neutrons respectively generated through deuterium-tritium (DT) and deuterium-deuterium (DD) fusion reactions. The architecture of the RNC (fig. 1) is based on two subsystems (figure 1) with collimating structure looking radially at the plasma by means of optical paths hollowed out of the EP01 Diagnostic First Wall (DFW) and Diagnostic Shielding Module (DSM) [2].

The in-port RNC enclosed in a stainless steel removable cassette equipped with electrical and vacuum feedthrough, is integrated in the DSM *Drawer #3* of the EP01. The neutrons coming from the plasma edges ($r/a > 0.67$, a = minor radius) are collected by means of two sets of three Lines of Sight (LoS) each and pass through the collimators up to the detector module containing two in-line devices: a single Crystal Diamond (sCD) 3x3

matrix as primary detector and a ^{238}U fission chamber (FC) as complementary one.

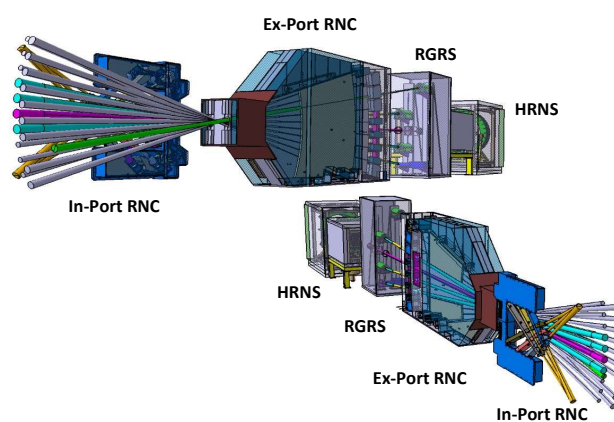


Fig. 1. ITER Radial Neutron Camera layout and interfacing diagnostic systems.

The ex-port RNC, which optical paths are located in the Port Plug in *Drawer #2*, is devoted to probe the plasma

core ($r/a < 0.54$) and consists of a massive shielding block, extending from the Port Interspace to the Bioshield Plug that encompasses 16 interleaved LoS lying on different toroidal planes. The detector boxes, located at the end of the collimating structures, are equipped with plastic and Helium scintillators and diamond detectors. The ex-port RNC interfaces with the High Resolution Neutron Spectrometer and the Radial Gamma Ray Spectrometer which have 1 and 3 dedicated LoS respectively (four central collimators of the right set, looking towards the plasma).

The direct DT and DD neutrons passing through the DFW and DSM cut-outs and reaching the detectors through the collimators, allow the measurement of the neutron emissivity and α -source profile as well as the relative fusion power density by means of the application of specific reconstruction algorithms to the line-integrated neutron fluxes. Moreover, the RNC is designed to provide the core ion temperature profile and the assessment of the fuel ratio [3,4].

The reliability and effectiveness of the RNC detection system relies, among other aspects related to the efficiency of the detection system, on the capability to amplify the low amplitude signals coming from the sCDs, scintillators and FCs and, at the same time, to minimize their degradation. For this purpose, front-end electronics (i.e. preamplifiers) have to be located as close as possible to the detectors, in order to avoid spurious signals collected in the cabling assembly. On the other hand, the electronic devices have to withstand a severe radiation environment during normal operating conditions (NOC) due to the intense neutron streaming directly from the plasma and the effects of secondary gammas generated through the interaction of neutrons with the surrounding machine components. The most common mitigation strategies to ensure a proper functioning of the equipment are the following: i) planned replacement of the damaged instrumentation, ii) positioning in shielded areas where the compliancy with the alert thresholds in terms of neutron fluence and cumulated ionizing dose is satisfied, iii) development of dedicated shielded cabinets that can adequately protect the devices.

The closest possible location for the RNC electronics is in the Port Cell, close to the ex-port shielding unit (figure 2), about 8.5 mt away from the in-port detector. In this area, a significant radiation level is present because of the proximity to the Bioshield plug that hosts several penetrations dedicated to feedthroughs, cooling pipes and diagnostics. Taking into account these issues, the solution proposed to ensure a suitable protection for the ITER RNC preamplifiers relies on conceiving a cabinet layout that could ensure the necessary magnetic, thermal and nuclear shielding and, at the same, satisfy weight and allocated volume constraints and maintain its structural integrity.

2. Nuclear design of a shielded cabinet for the RNC preamplifiers

The layout for the RNC preamplifiers shielded cabinet (figure 3) is based on a multi-layer concept summarised in Tab. 1. In order to achieve an efficient protection of the inner electronic components neutron and gamma radiation and electromagnetic fields, a specific layered design has been developed for EU21 side and top/bottom walls which are enclosed in a Stainless Steel (SS316L(N)-IG) external case.

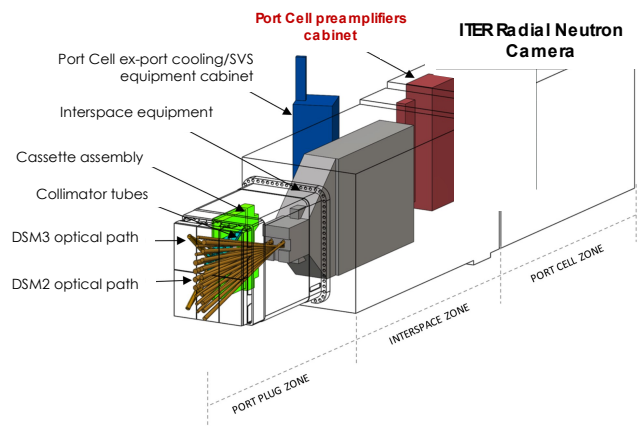


Fig. 2. Overview of the ITER Radial Neutron Camera structure and location of the shielded cabinet for preamplifiers.

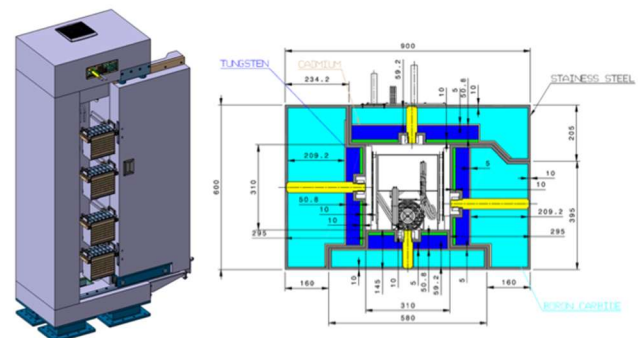


Fig. 3. Overview of the ITER RNC shielded cabinet for preamplifiers (left picture) and section showing the inner layered structure (right picture).

Table 1. Shielded Cabinet structure description. Each layer is enclosed in a SS316L(N)-IG external case.

Cabinet side	Material	Thickness (cm)	Role
Left hand side and right hand side	Boron Carbide (B ₄ C)	5	Fast neutron moderator
Front and back		20	
All sides	Cadmium (Cd)	0.5	Thermal neutrons absorber
All sides	Tungsten (W)	7	Gamma attenuation
All sides	Ferromagnetic alloy	2	Electromagnetic shielding

As mentioned above, the shielded cabinet will be exposed to a significant radiation field (up to $\sim 4 \times 10^5$ n/cm²/s) thus an outer Boron Carbide (B₄C) layer has been placed on all sides with the aim of moderating the fast neutron flux that mainly arises out of the Bioshield plug; in order to enhance the neutron shielding effectiveness, the front side of the cabinet, oriented towards the Bioshield, has been equipped with a thicker B₄C slab (20 cm). A second Cadmium layer has been immediately added after the B₄C slabs in order to absorb the residual thermal and epithermal neutrons. The driving physical phenomena through which the neutrons are moderated/absorbed are the (n,γ) reactions: consequently, the main drawback is the generation of a consistent gamma flux that need to be reduced in order to avoid potential harmful effects on the electronic equipment as well as the pile-up of spurious signal due to photons. For this purpose a 7 cm thick Tungsten layer has been added on all the sides as gamma attenuator. Finally, the electromagnetic compatibility is achieved through the integration of ferromagnetic slabs, which aim at shielding both the static magnetic field and the transient electromagnetic fields associated to events such as plasma disruptions, vertical displacement events and magnet current discharges.

3. Nuclear analyses

The proposed layout for the electronics shielded cabinet so far described underwent a specific nuclear analysis to verify its reliability in protecting the enclosed preamplifiers. A detailed MCNP [5] model of the cabinet has been generated through the conversion of a pre-processed engineering CAD model by means of the CAD-to-MCNP interface embedded in the SuperMC code [6] (figure 4).

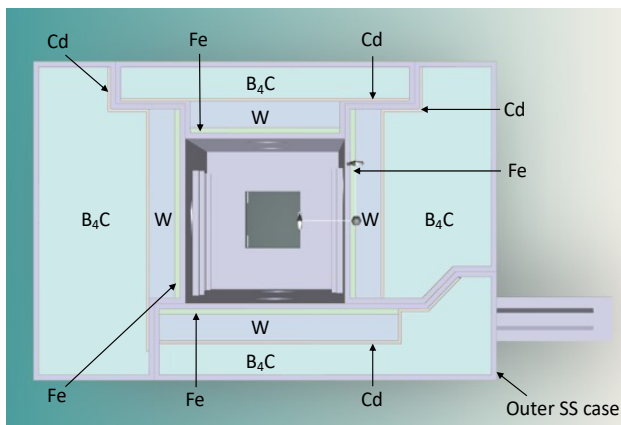


Fig. 4. Section of the MCNP model of the shielded cabinet for electronics showing the inner layered structure.

The MCNP model so far developed has been integrated into an extended version of the standard ITER reference neutronics model (C-model, release R181031, [7]) which includes the updated features and components of the Equatorial Port 01 (EP01, [8]) as well as the corresponding Port Cell (PC01, figure 5). It consists of a 40° regular sector of the machine, where the EP01 structure is enclosed in the two side half-port, while the central full-size equatorial is filled with a Diagnostic

Generic Equatorial Port Plug (DGEPP), with dummy DFW and DSM. Periodic boundary conditions are toroidally applied at the planes that delimit the sector, in order to properly simulate the whole tokamak. The model also includes material specifications for particle transport, making use of the FENDL-3.1d [8] nuclear data libraries. With respect to the analyses conducted for the In-port RNC [9,10], the EP01 structure has been split into the two peripheral half ports in order to take into account for the effect of the cross-talk from the Lower Port on the assessment of the nuclear loads in the Port Cell area (figure 6).

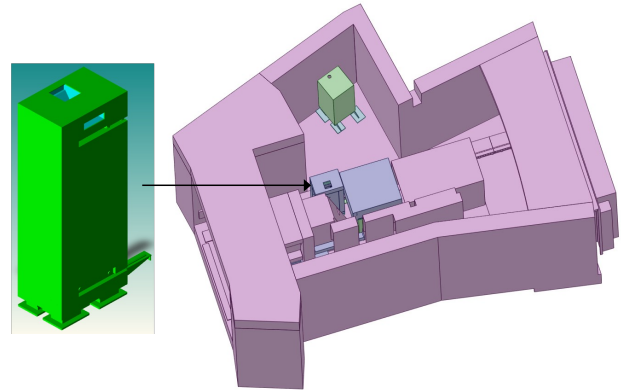


Fig. 5. Port Cell 01 MCNP model integrating the shielded cabinet for preamplifiers

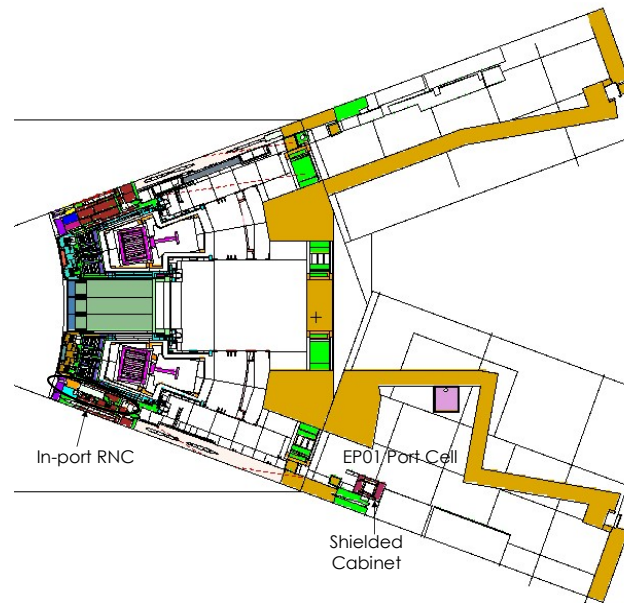


Fig. 6. Toroidal section of the ITER MCNP C-model integrating the EP01 features and the shielded cabinet in the PC01.

The extended and updated ITER C-model integrating the shielded cabinet in the PC01 has been used to assess specific nuclear loads (i.e. neutron and gamma flux spatial distribution, nuclear heating and cumulative dose to Silicon) aimed at verifying the shielding effectiveness of the cabinet. Calculations have been performed using the standard ITER plasma source provided with the C-model (inductive H-mode, 10 MA/5.3T, 500 MW fusion power, neutron rate: 1.773×10^{20} s⁻¹) and using mesh-based tallies,

considering 2 different voxels sizes (10 cm and 20 cm respectively). Proper tally multipliers, defined to take into account the involved materials and nuclear reactions, as well as the proper normalization factors have been set. From the computational point of view, the idea of transporting the neutrons directly from the plasma source up to the Port Cell is quite a challenging task: apart from the relative distance of the cabinet with respect to the Vacuum Vessel, the source neutrons flux is strongly moderated by the Bioshield Plug concrete through scattering phenomena, so very few particles are likely to reach the scoring position. Moreover, due to the intrinsic nature of the cabinet, the neutrons and gammas that can reach the inner cavity and contribute to the tallies are quite rare. Taking into account these issues, the reliability of the numerical results (e.g. convergence or fluctuation criteria), ensuring relevance for the objectives of the nuclear analysis, is achieved through the application of proper variance reduction techniques. In this specific case, ‘weight windows’ [5] files have been developed for neutrons (figure 7) and photons (figure 8), by means of the Advantg hybrid code [11] and successively customized using the iWW-GVR tool [12].

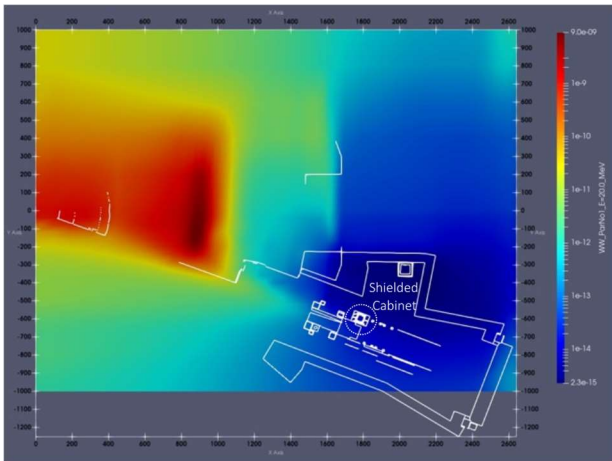


Fig. 7. Toroidal section of the weight windows file generated for neutrons. The shielded cabinet position is indicated by means of a dotted circle.

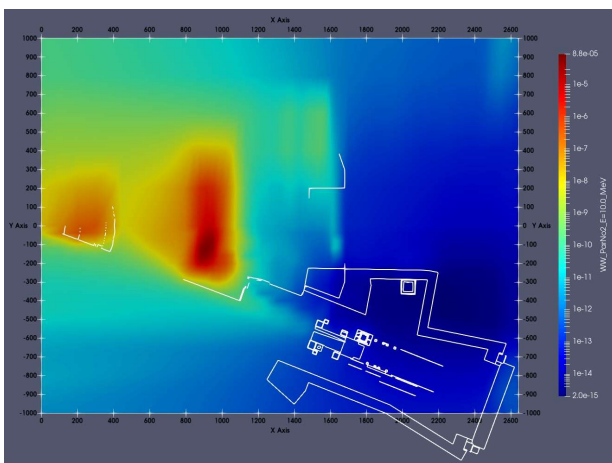


Fig. 8. Toroidal section of the weight windows file generated for photons. The shielded cabinet position is indicated by means of a dotted circle.

The usage of this technique guarantees statistically reliable results (i.e. statistical error on the investigated nuclear responses < 10%), allowing an efficient particle transport even through massive shielding components (e.g. Bioshield, ex-port RNC shielding unit).

3.1 Neutrons and photons spatial distribution

The total neutron flux spatial distribution in 3D map format, extended from the Bioshield up to the Port Cell area is shown in figure 9: a variation of about 2 orders of magnitude has been assessed from the outer side of the shielded cabinet towards the Bioshield (yellow area in the plot, corresponding to a total neutron flux density up to 3.8×10^5 n/cm²/s) to the inner cavity (average neutron flux density: 3.6×10^3 n/cm²/s), thus highlighting the shielding effectiveness of the layered structure.

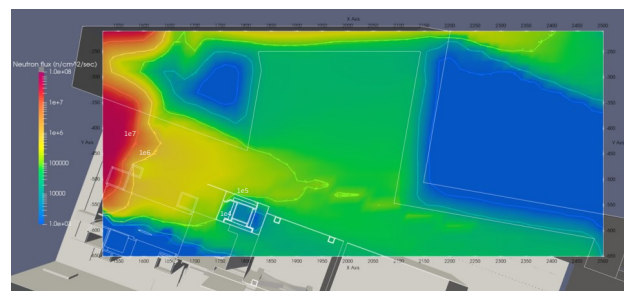


Fig. 9. Toroidal section of the total neutron flux (n/cm²/s) map across the shielded cabinet midplane.

Figure 10 shows a section of the neutron flux map along the cabinet longitudinal axis that allows an insight of the radiation field within. The neutron flux density inside the cavity is almost isotropic except for the lower area, where the neutron steaming through the air flow system penetration results in a locally increased neutron flux. Taking into account this issue, it would be preferable to locate the preamplifiers trays away from this zone: the average neutron flux density computed over the shielded cabinet inner space voxels decreases up to 2.5×10^3 n/cm²/s if the contribution from the lower zone of the cavity is excluded (i.e. computing the average neutron flux density considering the voxels from the lower tray fixations upwards).

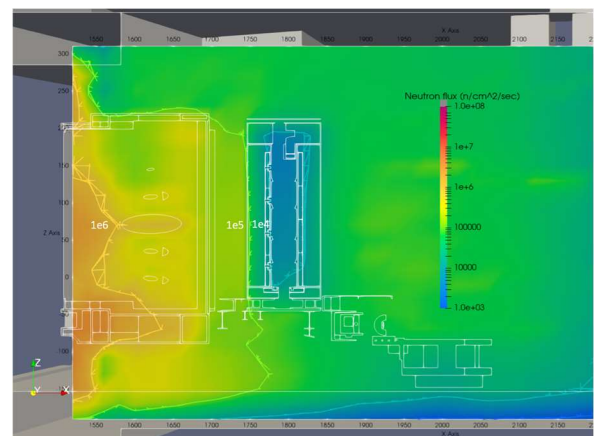


Fig. 10. Section of the total neutron flux (n/cm²/s) map across the shielded cabinet longitudinal axis.

The gamma flux maps are shown in figure 11 and figure 12 (toroidal section up to the Port Cell and detail of the EU21 though a section along its longitudinal axis, respectively). As for the neutrons, the shielded cabinet provides a significant gamma flux reduction: the gamma flux outside the cabinet, towards the Bioshield, is around $1.2 \times 10^5 \gamma/cm^2/s$ and decreases down to $1.15 \times 10^3 \gamma/cm^2/s$ inside it. With respect to the neutron flux density, the behavior of the gamma radiation field inside the inner space for electronics does not present a significant gradient along its longitudinal axis.

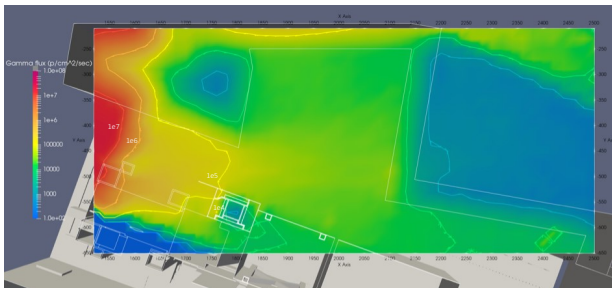


Fig. 11. Toroidal section of the gamma flux ($\gamma/cm^2/s$) map across the shielded cabinet midplane.

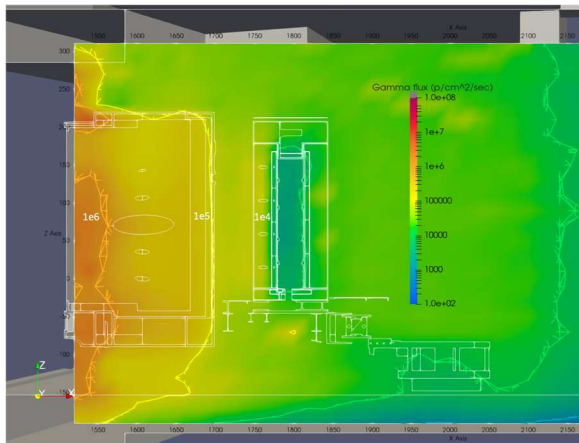


Fig. 12. Section of the gamma flux ($\gamma/cm^2/s$) map across the shielded cabinet longitudinal axis.

3.2 Nuclear heating

The nuclear heating density map has been computed taking into account both the contribution of neutrons and secondary gammas (figure 13): the average heat load inside the shielded cabinet inner cavity is $3.5 \times 10^{-11} W/cm^3$, where the available space has been filled with Silicon in order to simulate the electronic devices that will be hosted within. Table 2 summarizes the nuclear heating values assessed on the different layers of the structure: the average heat load deposited on the external stainless steel envelope is $7.4 \times 10^{-9} W/cm^3$, thus a reduction of more than two order of magnitude is achieved in the area where the preamplifiers will be installed.

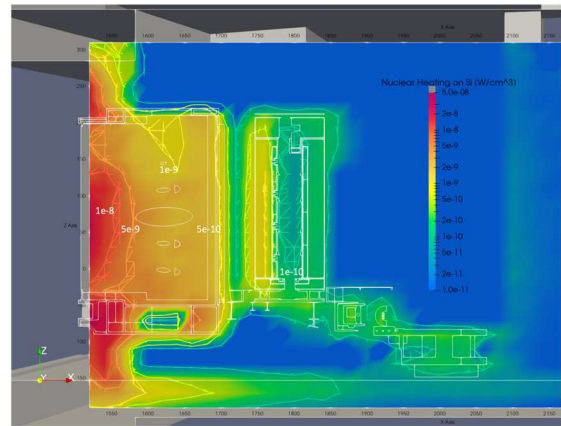


Fig. 13. Section of the nuclear heating (W/cm^3) map across the shielded cabinet longitudinal axis.

Table 2. Nuclear heating density assessed on the shielded cabinet layers.

Layer (material)	Nuclear heating density (W/cm^3)
External structure (stainless steel SS316L(N)-IG)	7.4×10^{-9}
Layer 1 (Boron Carbide)	1×10^{-9}
Layer 2 (Cadmium)	5×10^{-10}
Layer 3 (Tungsten)	5×10^{-10}
Layer 4 (Iron)	6×10^{-11}
Inner cavity (Silicon)	3.5×10^{-11}

3.3 Integrated dose to Silicon

The dose to Si has been assessed in order to verify the suitability of commercial or rad-hard electronics with the radiation environment inside the Shielded Cabinet cavity. Figure 14 shows a section of the dose to Si integrated over the ITER lifetime (1.7×10^7 seconds) 3D map, computed taking into account both the effect of neutrons and secondary gammas: the spatial distribution presents an increase in the upper and lower areas close to the air flow penetrations, while it is almost isotropic inside the cavity, with an average value around 1.5 Gy.

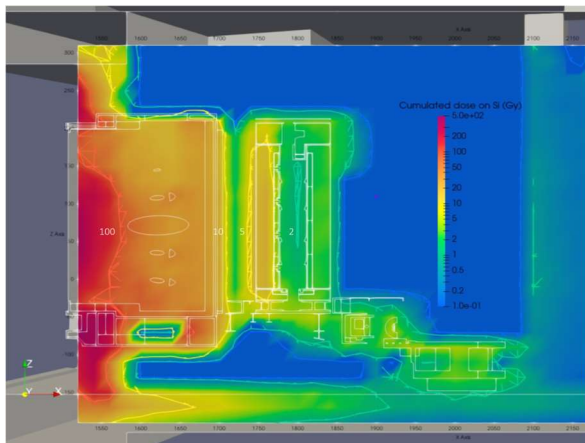


Fig. 14. Section of the integrated dose to Silicon (Gy) map across the shielded cabinet longitudinal axis.

3.4 Nuclear loads assessed in the shielded cabinet inner cavity

The 3D maps provide a useful overview of the radiation field and nuclear responses spatial distribution; however, for a more precise assessment of the average neutron/photon flux and dose to electronics devices, specific tallies (F4) has been set on the cells that define the actual space in cabinet dedicated to host the preamplifiers; moreover, proper multipliers considering the involved nuclear reactions, the ITER neutron yield and the specific material (Silicon) have been defined to evaluate the cumulative dose. The results are summarized in Table 3, where the shielding factors provided by the cabinet are reported as well.

Table 3. Nuclear loads assessed inside and outside the shielded cabinet for preamplifiers.

	Inside the cabinet	Outside the cabinet	Shielding factor
Neutron flux (n/cm ² /s)	3.6x10 ³	3.8x10 ⁵	1.06x10 ²
Gamma flux (γ/cm ² /sec)	1.15x10 ³	1.2x10 ⁵	1.04x10 ²
Integrated absorbed dose to Si (Gy)	1.5	N.A.	N.A.

The nuclear responses evaluated so far provide indications about the cumulative effects of radiation streaming inside the shielded cabinet; however, the neutron flux impinging on electronic devices could randomly provoke instantaneous dysfunctions or failure through a mechanism defined as Single Event Effect (SEE, [13]). The estimation of a SEE rate relies on the assessment of the neutron spectrum computed at the location of the equipment and the cross section of production of the given SEE by neutrons for the considered device ($\sigma^{SEE}(E)$). The determination of the $\sigma^{SEE}(E)$ for a specific energy range is carried out by a set of measurement under mono-energetic neutrons that are out of the scope of the present analysis. Nevertheless, the average neutron spectrum at the preamplifiers position is

provided in figure 15: it confirms the shielding effectiveness of the shielded cabinet layered structure that ensures a flux lower than 10 neutrons/cm²/s in the energy range between 1 and 14 MeV, while the thermal component is below 2.1x10² neutrons/cm²/s. A 3D map of the fast ($E > 100$ keV) neutron flux inside the cabinet (figure 16) highlights that the average fast neutron flux in the inner cavity is around 2x10² neutrons/cm²/s. Even if the layered structure provides a significant reduction of the nuclear loads on the electronic equipment with respect to the external environment, the usage of rad-hard electronics is recommended in order to ensure a proper operation of the devices during the ITER experimental campaigns.

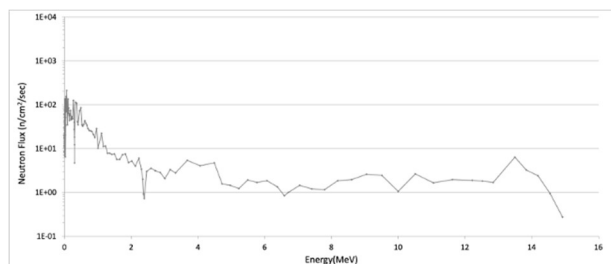


Fig. 15: Neutron spectrum computed inside the shielded cabinet at the preamplifiers location.

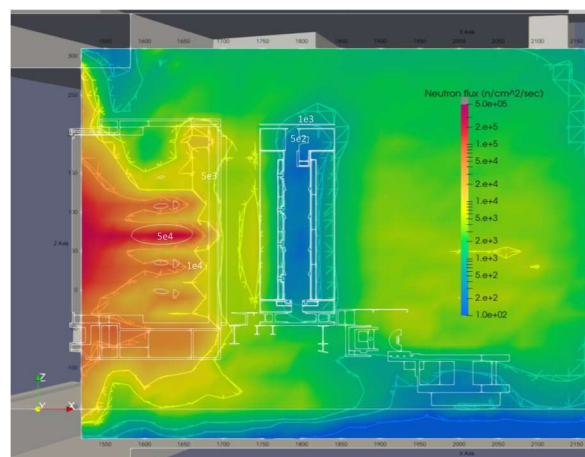


Fig. 16. Section of the fast ($E > 100$ keV) neutron flux (n/cm²/s) map across the shielded cabinet longitudinal axis.

4. Conclusions

The estimation of line-integrated neutron flux and spectra performed by means of the RNC has a paramount impact on the successful exploitation of the ITER experimental campaigns since it allows to investigate several key parameters for the assessment of the total fusion power as well as for plasma control and plasma physics analyses. As a matter of fact, the effectiveness of the measurements relies on the proper functioning of the front-end electronics that have to withstand a severe environment in terms of radiation streaming and magnetic fields in the EP01 Port Cell. For this purpose, a dedicated shielded cabinet has been developed, taking into account the space and weight constraints, with the aim of reducing the effects of neutron and gamma radiation on the detectors preamplifiers that will be hosted inside it.

A comprehensive nuclear analysis has been conducted for the RNC shielded cabinet, providing the average neutrons/photons flux and dose to Si, simulating the inner electronic devices, as well as the 3D spatial distribution of the above-mentioned nuclear responses. The results obtained for the EP01 Port Cell are coherent with the latest analyses released by the ITER Organization (IO) aimed at the characterization of radiation environment for equipment during operations [14].

The results highlight that the shielded cabinet structure provides a substantial reduction of the nuclear loads (about a factor 100 for both the neutron and gamma fluxes), with respect to the surrounding environment, taking into account the penetrations present in the Bioshield plug that contribute to increase the neutron streaming in the Port Cell area. In particular (Table 4), the absorbed dose to Si integrated over the ITER lifetime is 3 Gy, below the alert threshold for commercial electronics [15]. On the other hand, the neutron flux is still 2 orders of magnitude larger than the alert threshold. Based on these results, the RNC preamplifiers should be designed and tested in compliance with such neutron flux, in order to guarantee a proper functioning during plasma operations.

Table 4. Comparison between the nuclear loads assessed inside the shielded cabinet (including a safety factor '2' as foreseen by IO [14]) vs alert thresholds for the usage of commercial electronic devices.

Nuclear response	Average values inside the shielded cabinet with safety factor	Alert threshold for commercial electronics
Neutron flux (n/cm ² /s)	7.2x10 ³	10 ²
Integrated absorbed dose to Si (Gy)	3	10

References

- [1] B. Esposito, et al., 'Progress of Design and Development for the ITER Radial Neutron Camera', *Journal of Fusion Energy*, vol. 41, issue 2, article number 22, 2022.
- [2] D. Marocco et al., 'System level design and performances of the ITER radial neutron camera', *Proceedings of the 26th IAEA Fusion Energy Conference, Kyoto*, 2016.
- [3] D. Marocco et al., 'Combined unfolding and spatial inversion of neutron camera measurements for ion temperature profile determination in ITER', *Nuclear Fusion*, vol 51, Art. no. 053011, 2011.
- [4] D. Marocco et al., 'Neutron measurements in ITER using the Radial Neutron Camera', *Journal of Instrumentation*, vol. 7, no. 3, Art. no. C03033, 2012.
- [5] *X-5 Monte Carlo Team: MCNP - A General Monte Carlo N-Particle Transport Code, Version 5*, LANL Report: LACP-03-0245, 2005.
- [6] Y. Wu, FDS Team, 'CAD-based interface programs for fusion neutron transport simulation', *Fusion Engineering and Design*, vol. 84, pp. 1987-1992, 2009.
- [7] D. Leichter et al., 'The ITER tokamak neutronics reference model C-Model', *Fusion Engineering and Design*, vol. 136, pp. 742-746, 2018.
- [8] *FENDL-3.1d: Fusion Evaluated Nuclear Data Library ver:3.1d*, <https://www-nds.iaea.org/fendl/>, 2018.
- [9] F. Moro et al., 'Nuclear analyses for the assessment of the loads on the ITER Radial Neutron Camera in-port system and evaluation of its

measurement performances', *IEEE Transactions on Plasma Science*, doi: 10.1109/TPS.2022.3185801, 2022

- [10] F. Moro et al., 'The ITER radial neutron camera in-port system: Nuclear analyses in support of its design development', *Fusion Engineering and Design*, vol. 146, pp. 236-241, 2019.
- [11] W. Mosher et al. ADVANTG - An Automated Variance Reduction Parameter Generator, ORNL/TM 2013/416 Rev. 1. Technical report, Oak Ridge National Laboratory, 2015
- [12] M. Fabbri, Á. Cubi, iWW-GVR: A tool to manipulate MCNP weight windows (WW) and to generate Global Variance Reduction (GVR) parameters
URL: <https://github.com/Radiation-Transport/iWW-GVR>
- [13] M. Dentan, 'Overview of the ATLAS policy on radiation tolerant electronics', *Proceedings of '6th Workshop on Electronics for LHC Experiments'*, pp 270-274, doi: 10.5170/CERN-2000-010.270, 2000
- [14] Radiation environment for equipment during operations (ITER_D_3FM25L v1.1).
- [15] Proposed Strategy for Electronics Exposed to Nuclear Radiations in ITER (ITER_D_QXPP97 v2.8).